Available online at www.sciencedirect.com

SciVerse ScienceDirect

Journal of Nutritional Biochemistry 23 (2012) 27–38

Journal of Nutritional Biochemistry

Medicarpin, a legume phytoalexin, stimulates osteoblast differentiation and promotes peak bone mass achievement in rats: evidence for estrogen receptor β-mediated osteogenic action of medicarpin

Biju Bhargavan[a,1], Divya Singh[a,1], Abnish K. Gautam[a,1], Jay Sharan Mishra[b,1], Amit Kumar[c], Atul Goel[c], Manish Dixit[c], Rashmi Pandey[a], Lakshmi Manickavasagam[d], Shailendra D. Dwivedi[b], Bandana Chakravarti[a], Girish K. Jain[d], Ravishankar Ramachandran[e], Rakesh Maurya[c], Arun Trivedi[b], Naibedya Chattopadhyay[a,*], Sabyasachi Sanyal[b,*]

[a]Division of Endocrinology, Central Drug Research Institute (Council of Scientific and Industrial Research), Chattar Manzil, P.O. Box 173, Lucknow, India
[b]Division of Drug Target Discovery and Development, Central Drug Research Institute (Council of Scientific and Industrial Research), Chattar Manzil, P.O. Box 173, Lucknow, India
[c]Division of Medicinal and Process Chemistry, Central Drug Research Institute (Council of Scientific and Industrial Research), Chattar Manzil, P.O. Box 173, Lucknow, India
[d]Division of Pharmacokinetics and Metabolism, Central Drug Research Institute (Council of Scientific and Industrial Research), Chattar Manzil, P.O. Box 173, Lucknow, India
[e]Division of Molecular and Structural Biology, Central Drug Research Institute (Council of Scientific and Industrial Research), Chattar Manzil, P.O. Box 173, Lucknow, India

Received 8 July 2010; received in revised form 11 October 2010; accepted 19 November 2010

Abstract

Dietary isoflavones including genistein and daidzein have been shown to have favorable bone conserving effects during estrogen deficiency in experimental animals and humans. We have evaluated osteogenic effect of medicarpin (Med); a phytoalexin that is structurally related to isoflavones and is found in dietary legumes. Med stimulated osteoblast differentiation and mineralization at as low as 10^{-10} M. Studies with signal transduction inhibitors demonstrated involvement of a p38 mitogen activated protein kinase-ER-bone morphogenic protein-2 pathway in mediating Med action in osteoblasts. Co-activator interaction studies demonstrated that Med acted as an estrogen receptor (ER) agonist; however, in contrast to 17β-estradiol, Med had no uterine estrogenicity and blocked proliferation of MCF-7 cells. Med increased protein levels of ERβ in osteoblasts. Selective knockdown of ERα and ERβ in osteoblasts established that osteogenic action of Med is ERβ-dependent. Female Sprague–Dawley (weaning) rats were administered Med at 1.0- and 10.0 mg.kg^{-1} doses by gavage for 30 days along with vehicle control. Med treatment resulted in increased formation of osteoporgenitor cells in the bone marrow and osteoid formation (mineralization surface, mineral apposition/bone formation rates) compared with vehicle group. In addition, Med increased cortical thickness and bone biomechanical strength. In pharmacokinetic studies, Med exhibited oral bioavailability of 22.34% and did not produce equol. Together, our results demonstrate Med stimulates osteoblast differentiation likely via ERβ, promotes achievement of peak bone mass, and is devoid of uterine estrogenicity. In addition, given its excellent oral bioavailability, Med can be potential osteogenic agent.

Keywords: Bone anabolic; Selective estrogen receptor modulator; Oral pharmacokinetics; Bone morphogenetic protein; Uterine estrogenicity; Bone microarchitecture; Bone strength

1. Introduction

The risk of osteoporotic fracture is most importantly dependent on biomechanical strength of bone [1–5]. Bone mass (a measure of bone size and its volumetric mineral density) is an established determinant of bone strength. Bone mass and strength achieved at the end of the growth period, commonly designated as peak bone mass (PBM), plays an important role in the risk of osteoporotic fractures occurring in adulthood. It is considered that an increase of PBM by one standard deviation may reduce the fracture risk by 50% [1]. Prevalence of low PBM in developing countries is often attributed to nutritional deficiency and significantly contributes to osteoporosis burden in population [6].

Phytoestrogens, found in many edible plants are diverse groups of biologically active compounds with structural similarity to estradiol [7]. The major phytoestrogens include daidzein and genistein that have been shown to reduce bone loss associated with estrogen deficiency in animals [8]. Perinatal exposure to phytoestrogens has been reported to lead to a higher bone mineral density later in life [9],

* Corresponding author: Naibedya Chattopadhyay is to be contacted at Division of Endocrinology, Central Drug Research Institute, M.G.Marg, Lucknow – 226 001, India. Tel.: +91 522 2613894; fax: +91 522 2623938, Sabyasachi Sanyal, Division of Drug Target Discovery and Development Central Drug Research Institute, M.G.Marg, Lucknow – 226 001, India.
E-mail addresses: n_chattopadhyay@cdri.res.in (N. Chattopadhyay), sanyal@cdri.res.in (S. Sanyal).
[1] Authors contributed equally to this work.

0955-2863/$ - see front matter © 2012 Elsevier Inc. All rights reserved.
doi:10.1016/j.jnutbio.2010.11.002

thus suggesting the potential for nutritional supplement of phytoestrogens. However, the effect of phytoestrogens in PBM achievement has not been investigated in detail.

The possibility of prophylactic as well as therapeutic uses of phytoestrogens in bone health is under active investigation [10], particularly in relation to the beneficial effect of consuming soy-rich food on bone health in Chinese women [11]. However, the effectiveness of soy isoflavones in skeleton is dependent on the production of an estrogenic metabolite, equol by a gut microflora, which is absent in almost 40% humans studied, thereby hindering the efficacy of soy isoflavones in humans [12–14]. In addition, results of recent clinical studies on the effect of soy isoflavones in affording bone conserving effects in postmenopausal osteoporosis was not convincing [15–17], thereby leaving the scope for identifying more effective forms of phytoestrogen/s for better bone health.

Although isoflavones are primarily known to signal via estrogen receptors (ERs), the role of ER subtypes (ERα and ERβ) in osteoblast function is unclear. It is generally thought that the major role of 17β-estradiol (E2) is to inhibit bone resorption, in part by stimulating osteoclast apoptosis [18]. The role of E2 in osteoblast and osteocyte functions has been demonstrated in mice using ERα knockout model. Mice lacking ERα have been shown to have defects in bone formation induced by mechanical stimulation, while, ERβ knockout mice did not show any bone phenotype [19]. However, both ERα and ERβ have been shown to express in osteoblasts and osteocytes [20], indicating that ERβ may have roles in osteoblast function.

Medicarpin (Med), 3-hydroxy-9-methoxypterocarpan, is a pterocarpan-type phytoalexin which is also classified as methoxylated isoflavonoid and is one of the major constituents of dietary legumes. Med is present in chickpea (*Cicer arietinum*) [21–23], *peanut (Arachis hypogaea*) [24], alfalfa (*Medicago sativa*) [25,26], red clover (*Trifolium pratense*) [27] and in an Indian medicinal plant *Butea monosperma* [28]. Recently, we have shown bone sparing action of Med under estrogen deficiency, suggesting an estrogen-"like" effect of Med in bone. Here, we investigated the effect of Med in rat skeletal growth (achievement of PBM), osteoblast function and molecular mode of action, and systemic bioavailability.

2. Materials and methods

2.1. Materials

Medicarpin was synthesized following our previously published protocol [29]. Cell culture media and supplements were purchased from Invitrogen (Carlsbad, CA, USA). All fine chemicals and inhibitors (ICI182780, U0126, SB203580, SP600125 and LY294002) were purchased from Sigma Aldrich (St. Louis, MO, USA). p38 mitogen-activated protein kinase (MAPK) enzyme-linked immunosorbent assay (ELISA) kit was purchased from Cell Signaling Technologies, Irvine, CA, USA. ECL kit was purchased from GE Healthcare Life Sciences, USA. ERα (2Q418): sc-71064 and ERβ (H-150): sc-8974 antibodies were from Santa Cruz Biotechnology, Santa Cruz, CA, USA. Progesterone receptor was (Santa Cruz), Bone morphogenetic protein-2 (BMP-2) ELISA (RnD systems, Minneapolis, MN, USA). Nonsilencing control (siC), ERα and ERβ siRNAs and corresponding transfection reagent Dharmafect I were purchased from Thermo Scientific, Waltham, MA, USA.

2.2. Plasmids

pM (contains yeast Gal4 DBD) and pVP16 (contains simian virus VP16 activation domain) were from Clontech. VP16-VDR was a kind gift from Dr. Makoto Makishima, Division of Biochemistry, Nihon University School of Medicine, Chiyoda, Tokyo, Japan. VP16-PRA and PRB were kind gifts from Dr. Stephen Lye, Departments of Obstetrics and Gynecology and Physiology, University of Toronto, Ontario, Canada. All other pM and VP16 constructs used in this study are described elsewhere [30,31]. Estrogen responsive elements (ERE)-Luc, pcDNAERα and pcDNAERβ were kind gifts from Dr. Eckardt Treuter, Department of Biosciences at Novum, Karolinska Institutet, Stokholm, Sweden. BRE-Luc was constructed using oligo cloning where 3×BRE sequence from ID-1 promoter was cloned into PGL3 promoter vector (Promega).

2.3. Culture of calvarial osteoblasts

Rat calvarial osteoblasts were obtained following our previously published protocol of sequential digestion [32–36]. Briefly, calvariae from 1–2-day-old Sprague–Dawley rats (both sexes) were pooled. After surgical isolation from the skull and the removal of sutures and adherent mesenchymal tissues, calvariae were subjected to

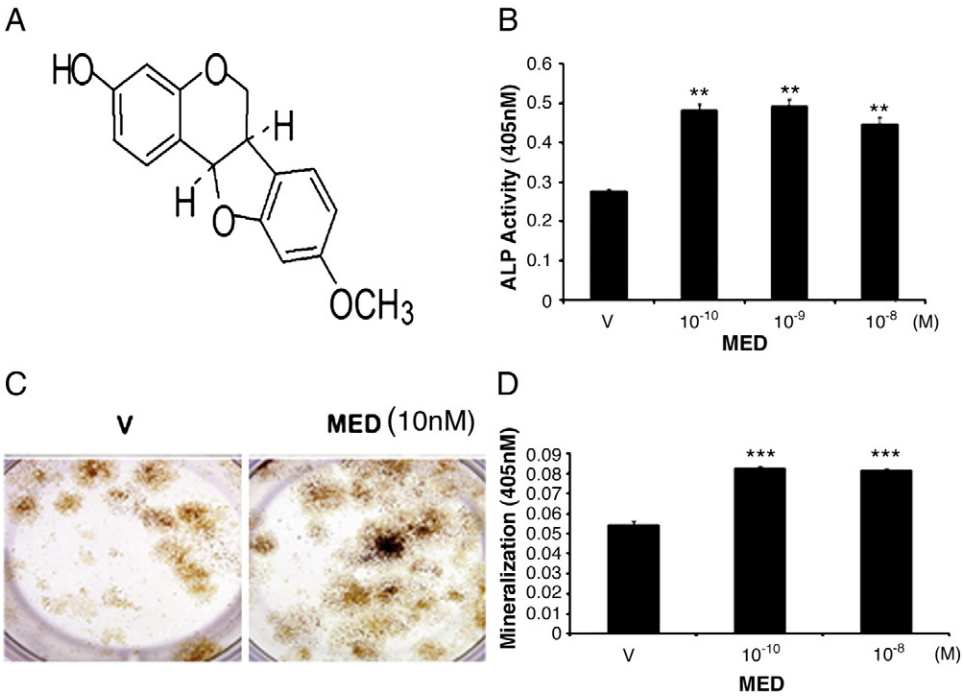

Fig. 1. Med stimulates osteoblast differentiation in vitro. (A) Structure of Med (3-hydroxy-9-methoxypterocarpan; ±-*cis*-medicarpin). (B) RCOs (2×10^3 cells/well) were seeded in 96-well plates. Cells were treated with various concentrations of Med for 48 h in osteoblast differentiation medium. ALP production was measured using a kit. (C) RCOs (2.5×10^3 cells/well) in 12-well plates were treated similarly as described in Panel B. Cultures were continued for 21 d with vehicle or Med and were stained with alizarin red-S. Stain was extracted and O.D. measured colorimetrically. Data shown as mean±S.E.M.; $n=3$; $^{**}P<.01$, $^{***}P<.001$ compared with vehicle (V)-treated cells.

five sequential (10–15 min) digestions at 37°C in a solution containing 0.1% dispase and 0.1% collagenase P. Cells released from the second to fifth digestions were pooled, centrifuged, resuspended and plated in T-25cm^2 flasks in α-minimal essential medium (α-MEM) containing 10% fetal calf serum (FCS) and 1% penicillin/streptomycin (complete growth medium).

2.4. Osteoblast differentiation and mineralization

For determination of alkaline phosphatase (ALP) activity, 2×10^3 cells per well were seeded in 96-well plates. Cells were treated with different concentrations of the compounds for 48 h in α-MEM supplemented with 5% charcoal treated FCS, 10 mM β-glycerophosphate, 50 μg/ml ascorbic acid and 1% penicillin/streptomycin (osteoblast differentiation medium). At the end of incubation period, total ALP activity was measured using *p*-nitrophenylphosphate as substrate and quantitated colorimetrically at 405 nm [32–35]. For mineralization studies, 2×10^3 cells per well were seeded in six-well plates in differentiation media with 10% charcoal treated FCS. Cells were cultured with and without the compound for 21 days at 37°C in a humidified atmosphere of 5% CO_2 and 95% air, and the medium was changed every 48 h. After 21 days, the attached cells were fixed in 4% formaldehyde for 20 min at room temperature and rinsed once in PBS. After fixation, the specimens were processed for staining with 40 mM alizarin red-S, which stains areas rich in nascent calcium.

For quantification of alizarin red-S staining, 800 μl of 10% (v/v) acetic acid was added to each well, and plates were incubated at room temperature for 30 min with shaking. The monolayer, now loosely attached to the plate, was then scraped with a cell scraper and transferred with 10% (v/v) acetic acid to a 1.5 ml tube. After vortexing for 30 s, the slurry was overlaid with 500 μl mineral oil (Sigma–Aldrich), heated to exactly 85°C for 10 min, and transferred to ice for 5 min. The slurry was then centrifuged at 20,000×*g* for 15 min and 500 μl of the supernatant was removed to a new tube. Then 200 μl of 10% (v/v) ammonium hydroxide was added to neutralize the acid. In some cases, the pH was measured at this point to ensure that it was between 4.1 and 4.5. OD (405 nm) of 150-μl aliquots of the supernatant were measured in 96-well format using opaque-walled, transparent-bottomed plates [28,32,33,37]. For studying cell signalling events, treatment of inhibitors (ICI182780, U0126, SB203580, SP600125 and LY294002) was given 30 min prior to the compound treatments.

2.5. Cell lines and reporter assays

COS-7 or HepG2 cells were maintained in Dulbecco's modified Eagle medium (DMEM) supplemented 10% fetal bovine serum (FBS). Twenty-four hours before transfection, cells were seeded onto 24-well plates in phenol-red free DMEM supplemented with 10% charcoal dextral treated FBS. Transfections were performed with Lipofectamine 2000 (Invitrogen) according to manufacturer's instructions. In all transfections, pEGFPC1 was used as an internal control. Total DNA in all transfections were kept constant at 700 ng/well using pcDNA3 empty vector. Following indicated treatments cells were lysed and relative luciferase values were determined using SteadyGlo kit (promega) in a GloMax luminometer (Promega). GFP expression in each well was quantitated by a multiplate fluorimeter (Polar Star Galaxy; BMG Labtech). Luciferase values were then normalized with GFP values and were plotted as fold activities over untreated controls or as indicated in the figures and legends.

2.6. siRNA transfection

Twenty four hours before transfection rat calvarial osteoblasts (RCOs) were plated in six-well plates in phenol red free medium supplemented with 10% charcoal dextran treated FBS. The cells were then transfected with 100 nM siC, siERα or siERβ using Dharmafect I transfection reagent (Dharmacon) following manufacturer's instructions. For quantitative polymerase chain reaction (qPCR) assays 16 h following transfection cells were treated with E2 or Med for 24 h followed by lysis in Trizol (Ambion) ,and for Western blotting, cells were treated with E2 or Med for 48 h, following which they were lysed in cell Lytic lysis buffer (Sigma).

2.7. RNA isolation and qPCR

Total RNA from each sample was isolated using Trizol (Ambion) according to manufacturer's instructions. Total RNA (1 μg) from each sample was reverse

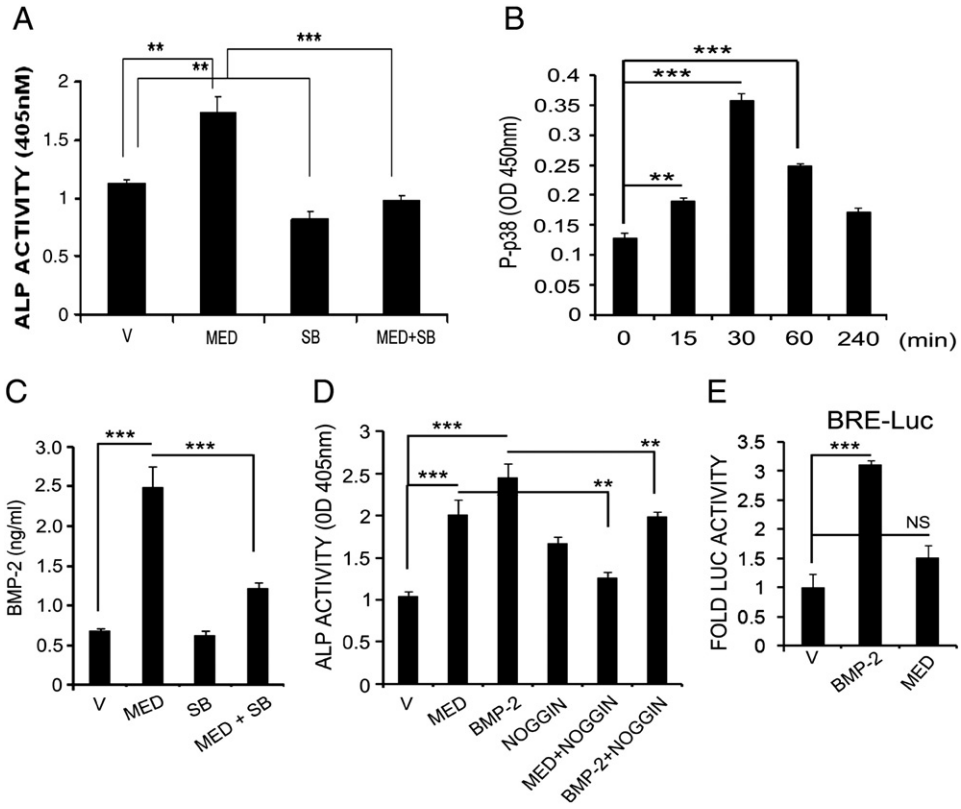

Fig. 2. Stimulation of osteoblast differentiation by Med requires activation of p38 MAPK and secretion of BMP-2. (A) RCOs (2×10^3 cells/well) were seeded in 96-well plates. Cells were first treated with 10 μM SB203580 (p38 MAPK inhibitor) for 30 min. Following PBS wash, Med (10 nM), with or without inhibitor was added in osteoblast differentiation medium. Cultures were continued for 48 h and ALP production measured. (B) RCOs (2×10^4 cells/well) were seeded in six-well plates and treated with 10 nM Med at different time points. Cell lysates were used to determine phospho-p38 MAPK and total p38 MAPK using ELISA kit. Phospho-p38 MAPK values are plotted after normalizing with total p38 MAPK. (C) RCOs (5×10^3 cells/well) were seeded in 24-well plates. Cells were treated with vehicle or Med (10 nM) or Med (10 nM)+10 μM SB203589 for 24 h. Supernatants were used for BMP-2 ELISA. (D) RCOs (2×10^3 cells/well) were seeded in 96-well plates. Cells were treated for 48 h with Med (10 nM), 100 ng/ml BMP-2 and 50 ng/ml noggin alone or in combination as described in the figure. ALP was measured. (E) HepG2 cells in 24-well plates were transfected with either 200 ng pcDNA3BMPR-Ia or 200ng of pcDNA3BMPR-II or 200ng BRE-Luc or 100ng EGFPC1. Sixteen hours following transfection, cells were treated with BMP-2 (100 ng/ml) or Med (10 nM) for 24 h, and then the cells were lysed, and luciferase activity was normalized against GFP and plotted as fold activity over untreated control. Data represent mean±S.E. from three independent experiments; $^{**}P<.01$, $^{***}P<.001$, NS, not significant.

transcribed using RevertAid First Strand cDNA Synthesis kit (Fermentas) according to manufacturer's instructions. mRNA levels of described genes were determined by SyBr green chemistry (Light Cycler 480 SyBr green I master; Roche) using a Light Cycler 480 (Roche) according to manufacturer's instructions. The specificity of the PCR product was documented by LightCycler melting curve analysis and migration on ethidium bromide-stained agarose gel. The relative quantitation for any given gene was calculated after determination of the difference between CT of the target gene and that of the calibrator gene glyceraldehyde-3- phosphate dehydrogenase (GAPDH) using a ΔCT method. Primer sequences for ER α (accession number: NM_012689.1) were 5′-GAT GGG CTT ATT GAC CAA CC-3′ (sense) and 5′-TGG AGA TTC AAG TTC CCA AA-3′ (antisense); for ER β (accession number: AB190769.1), 5′-CAA CCA GTG GCT GGG AGT-3′ (sense) and 5′-CAT GGG ACT CAG ATG TAA TGA CTG -3′ (antisense); for BMP-2 (accession number: NM_017178.1), 5′-CGG ACT GCG GTC TCC TAA-3′ (sense) and 5′-GGG GAA GCA GCA ACA CTA GA-3′ (antisense) and for GAPDH (accession number: AB017801.1), 5′-CAG CAA GGA TAC TGA GAG CAA GAG-3′ (sense) and 5′-GGA TGG AAT TGT GAG GGA GAT G-3′ (antisense).

2.8. Western blotting

Cells were grown to 60–70% confluence following which they were exposed to compounds for different time periods. The cells were then homogenized with triton lysis buffer (50 mM Tris-HCl, pH 8 containing 150 mM NaCl, 1% Triton X-100, 0.02% sodium azide, 10mM EDTA, 10 μg/ml aprotinin and 1 μg/ml aminoethylbenzenesulfonyl fluoride) and total proteins were quantified by Bradford method (Sigma). Thirty micrograms of total protein/sample was then resolved by 10% sodium dodecyl sulfate polyacrylamide gel electrophoresis (SDS-PAGE) and then transferred to polyvinylidene

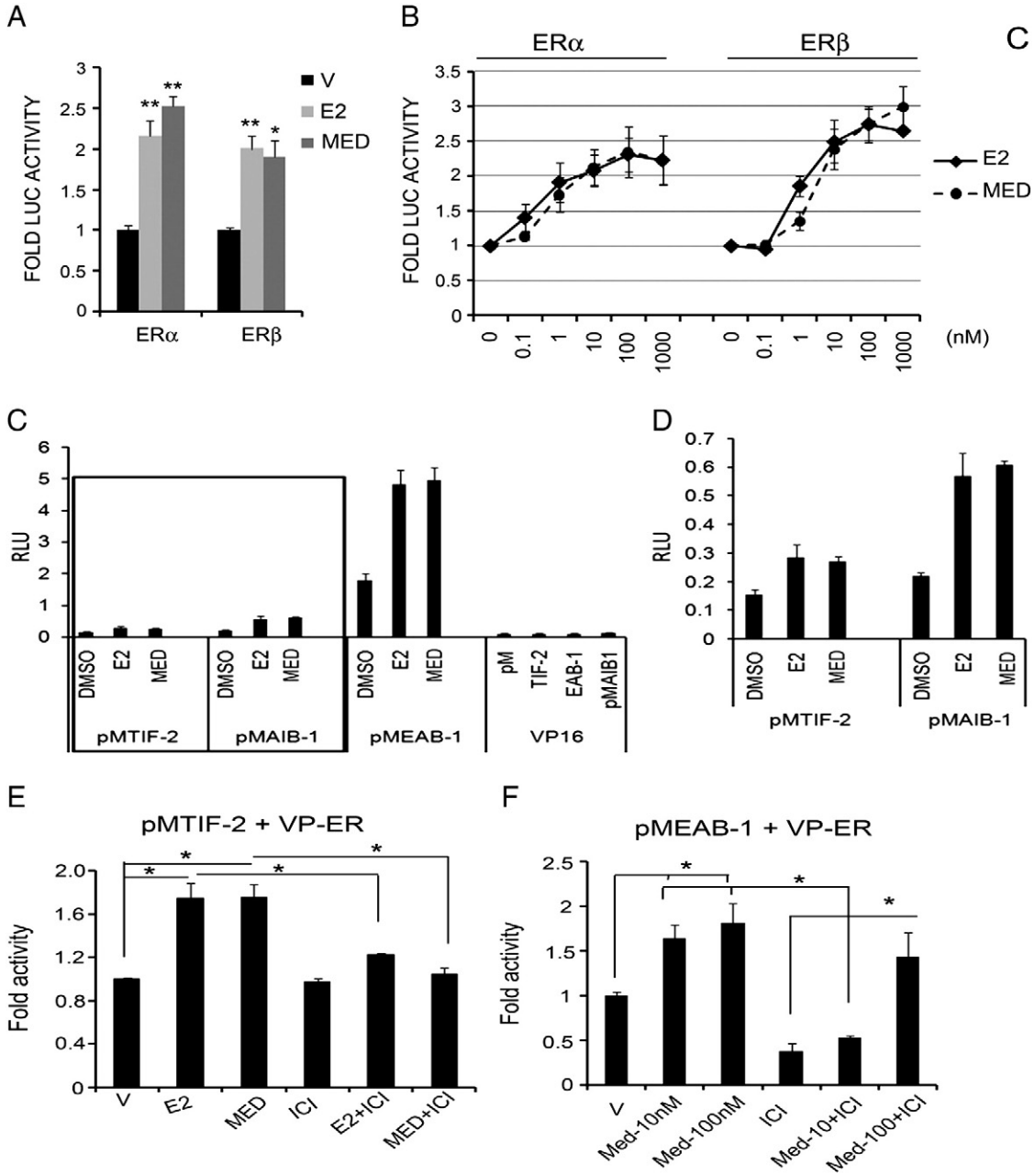

Fig. 3. Med transactivates ER in an ER negative, Cos-7 cells. (A) Cos-7 cells were transfected with 5×-GAL4-UAS-Luc, pMTIF-2 and VP16 ERα- or -β, and following indicated treatments (V, DMSO as vehicle; E2, 10 nM; Med, 10 nM), cells were lysed and luciferase assay was performed. (B) Cos-7 cells were transfected with 3×ERE-Luc, and indicated ER plasmids, following treatment with indicated concentrations of E2 or Med. Normalized luciferase activities were plotted as fold activity over vehicle-treated control. Data represent mean±S.E. from three independent experiments. (C) Cos-7 cells were transfected with VP16 empty vector/VP16-ERβ and pM-RID of TIF-2, AIB-1 or a synthetic ER-interacting peptide EAB-1 and following indicated treatments (DMSO as vehicle; E2, 10 nM and Med, 10 nM), normalized luciferase activities were plotted as relative light units (RLU). (D) Interactions of ER with pMTIF-2 and pMAIB-1 from panel C plotted separately. (E and F) Twenty-four hours following transfection of COS-7 cells with either pMTIF-2+VP-ER (E) or pMEAB+VP-ER (F), cells were treated with either E2 or Med for another 24 h. For ICI-182780 cotreatment, cells were pretreated with 10 nM ICI-182780 for 30 min. Normalized luciferase activity was plotted as fold activity over vehicle-treated cells. Data represent mean±SE from six independent experiments. *P<.05, **P<.01.

fluoride (PVDF) membranes (GE Healthcare). The membranes were incubated with different antibodies mentioned in figure legends followed by incubation with corresponding horseradish peroxidase-labeled secondary antibodies (Sigma). The bands were developed using ECL kit (Pierce).

2.9. p-38 MAPK ELISA

For measuring total and phospho-p38 MAPK, osteoblasts (20×10^3 cells/well) were seeded in six-well plates. Cells were exposed to Medicarpin for different time intervals (0, 15, 30, 60, 240 and 1440 min). Cells were lysed and proteins were quantified by Bradford method (Sigma). Total and phospho-p38 MAPK levels were determined by ELISA kit (Cell Signaling Technologies) following manufacturer's instruction. Inhibitor treatments were made as described in the figure legends [32,33].

2.10. In vivo experiments

The study was conducted in accordance with current legislation on animal experiments (Institutional Animal Ethical Committee) at Cental Drug Reserch Institute (CDRI). Twenty-four immature (21 days old) female Sprague–Dawley rats were used for the study [38]. All rats were housed at 21°C, in 12-h light:12-h dark cycles. Normal chow diet and water were provided ad libitum.

2.11. Assessment of various bone parameters

Rats were treated with 1.0- and 10.0-mg.kg^{-1} body weight doses of Med [29] or vehicle (gum acacia in distilled water) once daily for 30 consecutive days by oral gavage (eight rats/group). Each animal received intra-peritoneal injection of fluorochromes tetracycline (20 mg.kg^{-1} body weight dose) and calcein (20 mg.kg^{-1} body weight dose) on Days 15 and 28 of treatment, respectively. At autopsy, femora were dissected and separated from adjacent tissue, cleaned, fixed in 70% ethanol and stored at 4°C until further use. Initial and final body weight and uterine weight were recorded. Uteri were carefully excised, gently blotted, weighed and fixed for histology and histomorphometry as we reported earlier [32,33,35,39].

Bones were embedded in an acrylic material for the determination of bone formation rate (BFR), mineral appositional rate (MAR) and mineralization surface (MS). Fifty-micrometer sections were made using Isomet Bone cutter (Buehler, IL, USA), and photographs were taken under fluorescent microscope aided with appropriate filters. The calculations were done according to our previous reports [32,33,39,40].

Micro-computed tomography (μCT) determination of excised bones was carried out using the Sky Scan 1076 μCT scanner (Aartselaar, Belgium) as described in our previously published protocols [29,34,39]. Femurs and tibias were dissected from the animals after they were sacrificed, cleaned of soft tissue and fixed before storage in alcohol. The samples were scanned in batches of three at a nominal resolution (pixels) of 18 μm. Reconstruction was carried out using a modified Feldkamp algorithm using the Sky Scan Nrecon software, which facilitates network distributed reconstruction carried out on four personal computers running simultaneously. The X-ray source was set at 70 kV and 100 mA, with a pixel size of 18 μm. A hundred projections were acquired over an angular range of 180°. The image slices were reconstructed using the cone-beam reconstruction software version 2.6 based on the Feldkamp algorithm (Skyscan). Cortical thickness, cortical area, cortical perimeter, periosteal perimeter, periosteal perimeter and endosteal perimeter were calculated by 2D analysis of cortical bones of femur (mid-diaphysis).

After μCT measurements, femurs were subjected to three-point bending with bone strength tester Model TK 252C (Muromachi Kikai, Tokyo, Japan), according to our previously published protocols [32,34,35,41]. Biomechanical parameters of femur including maximum power, stiffness and energy were determined. Taking the mean of control values we derived individual control value as a ratio of the mean×100 and data expressed as percentage change over the mean value of sham group for the various biomechanical parameters.

For mineralization of bone marrow cells (BMCs) we followed our previously published protocol [32,33]. Briefly, femurs were excised aseptically, cleaned of soft tissues, and washed three times, 15 min each, in a culture medium containing 10 times the usual concentration of antibiotics as mentioned above. The epiphyses of femur were cut off and the marrow flushed out in 20 ml of culture medium consisting of α-MEM, supplemented with 15% charcoal treated FCS, 10^{-7} M dexamethasone, 50μg/ml ascorbic acid, and 10 mM β-glycerophosphate. Released BMCs were collected and plated (2×10^6 cells/well of six-well plate) in the culture medium, consisting of α-MEM, supplemented with 15% charcoal treated fetal bovine serum, 10^{-7} M dexamethazone, 50 μg/ml ascorbic acid, and 10 mM β-glycerophosphate. Cells were cultured for 21 days at 37°C in a humidified atmosphere of 5% CO_2 and 95% air, and the medium was changed every 48 h. After 21 days, the attached cells were fixed in 4% formaldehyde for 20 min at room temperature and rinsed once in PBS. After fixation, the specimens were processed for staining with 40 mM Alizarin Red-S, which stains areas rich in nascent calcium. Mineralization was quantified as describe above in material and method.

2.12. Assessment of uterine estrogenicity

Estrogen agonistic and antagonistic activities were evaluated as reported earlier from our laboratory [42]. Briefly, uteri were carefully dissected out, gently blotted, weighed, and fixed in 4% paraformaldehyde for histology, following our previously published papers [32,34,35,39]. About 5.0 mm pieces from the middle segment of each uterus were dehydrated in ascending grades of ethanol, cleared in xylene and embedded in paraffin wax using standard procedures. Representative transverse sections (5.0 μm) were stained with hematoxylin and eosin (H&E). Photomicrographs of sections were obtained using a Leica DC 300 camera and Leica IM50 Image Acquisition software fitted to a Leica DMLB microscope. The luminal epithelial height, luminal area and total uterine area were determined using the program Leica Qwin software (Leica Microsystems, Wetzlar, Germany).

2.13. Plasma pharmacokinetics

In vivo oral pharmacokinetic study was performed in female Sprague–Dawley rats (n=3, weight range 200–220 g). Med was administered a 5.0 mg.kg^{-1} bolus dose of Med by oral gavage. Blood samples were collected from the retro-orbital plexus of rats into microfuge tubes containing heparin as an anti-coagulant at 0.08, 0.25, 0.50, 1, 2, 4, 6, 8, and 10 h post-dosing. Plasma was harvested by centrifuging the blood at 13000 rpm for 10 min and stored frozen at −70±10°C until analysis. Plasma (100 μl) samples were spiked with IS (internal standard, 7-hydroxy isoflavone), and processed as described above. Along with the plasma samples, QC (quality control) samples were distributed among calibrators and unknown samples and analyzed by liquid chromatography mass spectrometry (LC MS/MS).

2.14. Statistics

Data are expressed as mean±S.E.M. The data obtained in experiments with multiple treatments were subjected to one-way analysis of variance followed by post hoc Tukey test of significance using MINITAB 13.1 software. Student's t test was used to study statistical significance in experiments with only two treatments.

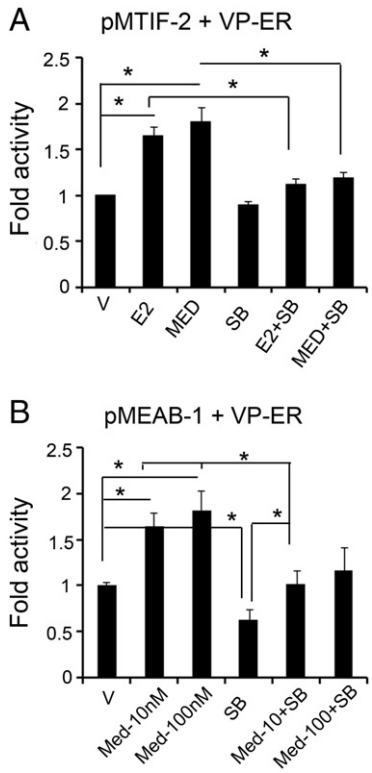

Fig. 4. Inhibition of p38 MAPK ameliorates Med and E2-induced ER–coactivator interaction. Twenty-four hours following transfection of COS-7 cells with either pMTIF-2+VP-ER (A) or pMEAB+VP-ER (B), cells were exposed to various treatments as indicated. For SB (SB203580) cotreatment, cells were pretreated with 10 μM SB203580 for 30 min. Normalized luciferase activity was plotted as fold activity over vehicle-treated cells. Data represent mean±S.E. from three independent experiments. *P<.05.

3. Results

3.1. Effects of Med on calvarial osteoblasts

Fig. 1A shows the chemical structure of Med (M.W. 270.2). To investigate the effect of Med in osteoblasts, RCO at >80% confluence was treated with Med (10^{-10} to 10^{-8} M), and as shown in Fig. 1B, Med stimulated ALP activity in osteoblasts, suggesting increased osteoblast differentiation. Med also stimulated mineralization of RCO strongly as demonstrated by alizarin red staining (Fig. 1C).

3.2. Effects of Med on p38 MAPK activation and BMP-2 secretion in osteoblasts

To investigate the mechanism of Med action in osteoblasts, we screened several signal transduction inhibitors to determine which inhibitor abolished Med action. We observed that the Med-induced ALP activity in RCOs was completely inhibited by p38 MAPK inhibitor SB203580 (Fig. 2A). Inhibitor of either p42/44 MAPK or jun-N-terminal kinase had no effect on Med-induced ALP production by osteoblasts (data not shown). Consistent with the observation that SB203580 blocked Med-induced ALP activity in osteoblasts, Med stimulated phosphorylation of p38 MAPK at 15 min, attaining peak phosphorylation at 30 min followed by a decline beyond 1 h (Fig. 2B). Since the expression of BMP-2, a potent stimulator of osteogenesis has previously been reported to be regulated by p38 MAPK pathway [43], we next investigated BMP-2 secretion in response to Med. As shown in Fig. 2C, BMP-2 levels in the conditioned medium were increased by Med treatment of osteoblasts. In addition, SB203580 significantly attenuated the Med-induced increase in BMP-2 secretion from osteoblasts (Fig. 2C). Further, noggin (an endogenous BMP-2 antagonist), blocked Med-induced ALP activity in RCO (Fig. 2D).

We next investigated if Med directly activated BMP receptor signaling. To that end, HepG2 cells were transfected with expression constructs for BMP receptors 1 and 2 and a corresponding BMP-response element-driven luciferase construct (BRE-Luc). Fig. 2E shows that although BMP-2 activated BRE-Luc activity in this assay system, Med failed to do so, indicating that Med is not a BMP receptor agonist. Together, data presented in Fig. 2 demonstrate that Med induces BMP-2 secretion via the p38 MAPK pathway in osteoblasts.

3.3. Characterization of ER activation and ER-coactivator interaction by Med

A previous report has demonstrated that BMP-2 is a transcriptional target for ER [44]. Since Med stimulated BMP-2 secretion via the activation of p38 MAPK in osteoblasts (Fig. 2), we carried out detailed investigation on the possible ER transactivation by Med. To that end, a low throughput screening was performed using a mammalian two hybrid interaction approach as reported earlier [30] in ER-negative COS-7 cells. As shown in Fig. 3A, Med specifically augmented VP16-ERα and -β interactions with yeast Gal4 DNA

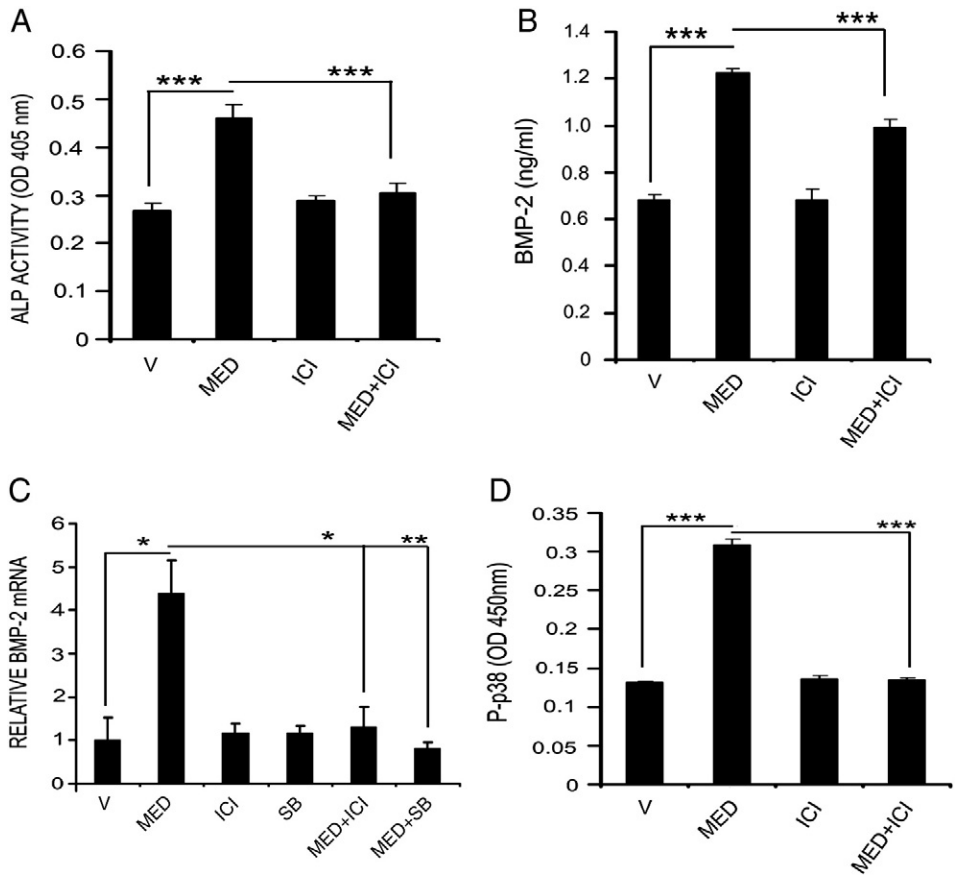

Fig. 5. Med stimulates osteoblast differentiation via ER and p38 MAPK. (A) RCOs were treated with either vehicle (V) or Med (10 nM) in the absence or presence of ICI (10 μM) and ALP activity was measured (as described in Fig. 1). (B) RCOs were cultured for 48 h in differentiation-inducing condition in 24-well plates. RCOs were exposed to various treatments as indicated and BMP-2 levels in the conditioned medium were measured by ELISA. (C) RCOs cultured similarly as in (B) and were exposed to various treatments as indicated. qRT PCR for BMP-2 mRNA was performed. (D) RCOs were exposed to various treatments as indicated for 30 min, following which protein lysate was prepared. Phospho-p38 MAPK was determined as described in Fig. 2B. Data represent mean±SE from three independent experiments. *P<.05; **P<.01; ***P<.001.

binding domain-fused receptor interaction domain (RID) of coactivator transcriptional intermediary factor-2 (TIF-2) (pMTIF-2), whereas it had no effect on coactivator interaction properties of a number of relevant nuclear receptors (supplementary Fig. S1). These results were also reproduced in HepG2 and Huh7 cell lines (data not shown). Med also concentration-dependently augmented ER activity on an ERE-driven luciferase reporter as potently as E2 (Fig. 3B). To further confirm the ER-modulating property of Med, ER interactions with yeast Gal4 DNA binding domain-fused RID of coactivator TIF-2, amplified in breast-1 (AIB-1), and a synthetic peptide that is reported to show E2-specific ER interaction, namely ER co-activater peptide (EAB-1) [31,45] were compared. Similar to E2, Med augmented ER interaction with all the RIDs (Fig. 3C, D). Interestingly, ER exhibited robust interaction with pMEAB-1 even in the absence of ER ligand and both E2 and Med further augmented this interaction (Fig. 3C and D).

Next, the effect of specific antiestrogen, ICI-182780 (ICI; to be used as ICI henceforth) on Med-induced ER-coactivator interactions in ER-negative Cos-7 cells transfected with exogenous ER was investigated. As shown in Fig. 3E, ICI alone had no effect on the basal reporter activity whilst ER–TIF-2 interaction induced by either E2 or Med was completely abolished in the presence of ICI. Further, ICI suppressed the ligand independent interaction between pMEAB-1 and ER, which Med was able to rescue in a concentration-dependent manner (Fig. 3F). Together, these data confirm transactivation of ER by Med in a heterologous system.

Since inhibiting p38 MAPK signaling abolished Med action in osteoblasts (shown in Fig. 2), the effect of SB203580 on Med-induced ER–coactivator interaction was investigated. In Cos-7 cells, SB203580 inhibited both E2- and Med-dependent ER–TIF-2 interaction (Fig. 4A). In addition, consistent with the data presented in Fig. 3F, ligand independent ER–EAB-1 interaction was inhibited by SB203580 and Med rescued the ER–EAB-1 interaction (Fig. 4B). These results demonstrate that Med acts via ER and p38 MAPK plays an integral role in Med-mediated ER activity.

3.4. Effect of Med in ER-regulated osteoblast functions

We next asked if the ER dependency of Med action in exogenous expression systems could be translated in osteoblasts. To that end, RCOs were treated with Med in the presence or absence of ICI. As shown in Fig. 5A, pretreatment with ICI abolished Med-stimulated ALP activity in RCOs. Also, ICI attenuated Med-stimulated BMP-2 release significantly from RCOs (Fig. 5B), suggesting ER-mediated function of Med in BMP-2 release from osteoblasts. We next studied whether Med has nuclear action in osteoblasts and to that end Med effect on BMP-2 mRNA levels was investigated in RCOs in the presence and absence of ICI and SB203580. As shown in Fig. 5C, Med treatment for 24 h resulted in robust increase in BMP-2 mRNA levels and the presence of either ICI or SB203580 completely abolished it, suggesting that the effect was mediated by ER-p38 MAPK pathway. Further, pretreatment of osteoblasts with ICI completely abolished stimulation of phosphorylation of p38 MAPK by Med (Fig. 5D).

We then studied the effect of Med and E2 in the expression of ERα and ERβ genes in RCOs. Consistent with previous reports [46], in RCOs, ERα protein was readily detectable whereas the abundance ERβ protein appeared low (Fig. 6A). Although basal (unstimulated) levels of ERβ protein were low in RCOs, both Med and E2 substantially increases protein levels of ERβ in RCOs but not ERα (Fig. 6A). From these data, it appears that ERβ could be involved in mediating osteogenic effect of Med.

To test the hypothesis that ERβ mediated the osteogenic effect of Med, we performed selective knockdown of ERα and ERβ in RCOs. Small interfering (si)ERα and siERβ reduced mRNA levels of the respective genes by 70% and 50% (Fig. 6B and C) and also efficiently reduced their respective protein levels (Fig. 6D). Fig. 6D

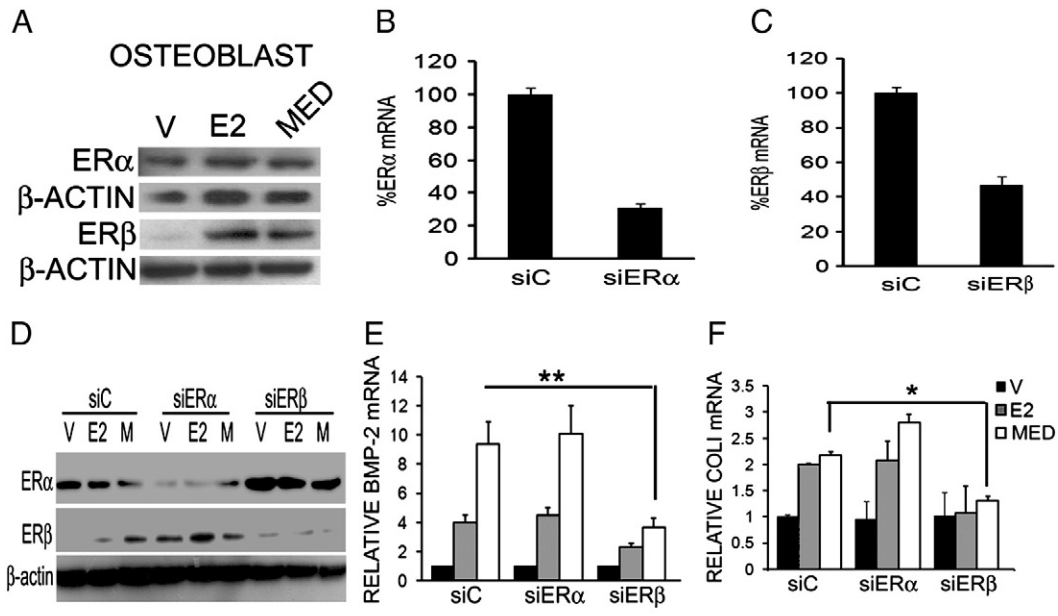

Fig. 6. Med induces osteogenic genes via ERβ up-regulation. (A) RCOs were treated with either vehicle (V, DMSO) or 10 nM E2 or 10 nM Med for 24 h. Western blot was performed with indicated antibodies. One representative result from two experiments with similar outcome is shown. (B and C) RCOs in six-well plates were transfected with 100 nM siC or siRNAs against ERα (B) and ERβ (C), using Dharmafect I transfection reagent according to manufacturer's instruction. Twenty-four hours after transfection, cells were lysed and mRNA levels of ERα (B) and ERβ (C) were determined by qRT-PCR. (D) RCOs were plated in six-well plates in triplicates. Sixteen hours after siRNA transfection, cells were treated with 10 nM E2 or Med for 48 h and cells were lysed. Lysates from three wells were pulled for each set 30 μg total protein for each set was resolved by 10% SDS-PAGE, followed by Western blot analysis. One representative blot out of two independent experiments with similar outcome is shown. (E and F) RCOs were plated in 6 well plates in triplicates. Sixteen hours following siRNA transfection, cells were treated with 10 nM E2 or Med for 48 h, and cells were lysed for extraction of total RNA. qRT-PCR was performed for quantitative determination of BMP-2 (E) and Type I collagen (COL I). (F) mRNA levels. Data (E,F) represent mean±S.E. from three independent experiments. *P<.05; **P<.01.

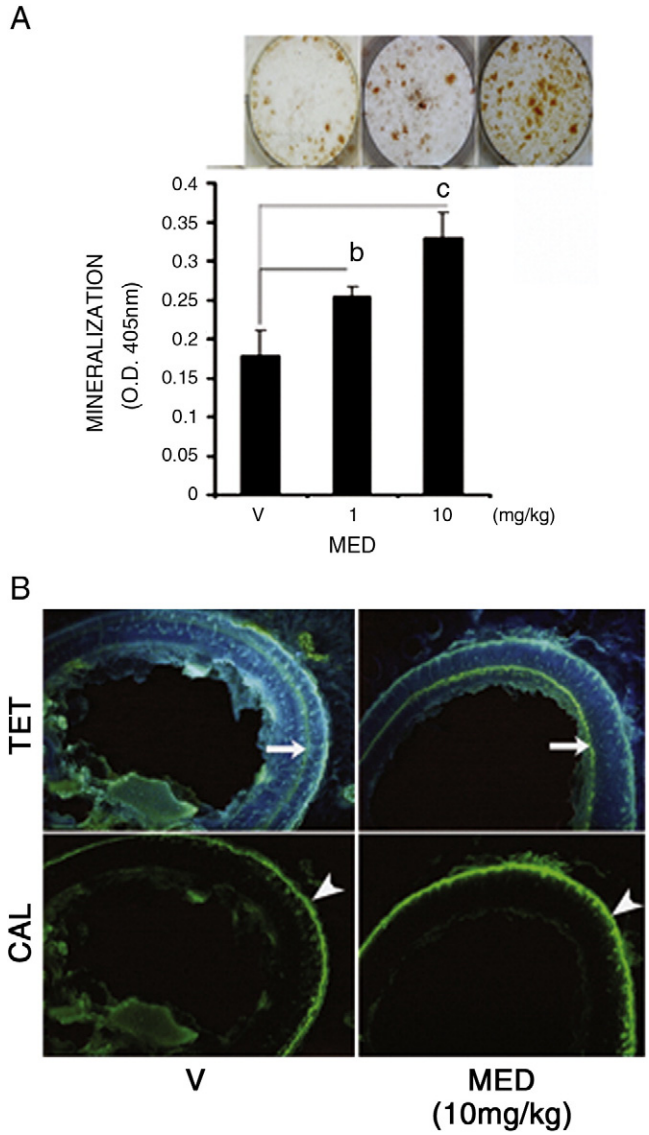

Fig. 7. Med has in vivo osteogenic effect. (A) 2×10^6 BMCs/well were plated onto 24-well plates from the V (vehicle control)- and Med-treated rats as described in Materials and methods. Cells were grown in osteoblast differentiation medium. Cultures were maintained for 21 d. Calcium deposition was determined by Alizarin Red-S staining of the cultures at the end of the experiment for all the groups. Top, Representative photomicrographs showing mineralized nodules in various groups. Bottom, Alizarin Red-S dye was extracted and quantified spectrophotometrically. Data represented as mean±S.E. $^{b}P<.01$, $^{c}P<.001$. (B) Following sequential tetracycline and calcein injections as described in materials and methods, rats were sacrificed and 50-μm sections of femur diaphysis of vehicle, and Med-treated rats were examined under fluorescent microscope. Representative photomicrographs of tertracyclin (ultraviolet filter) and calcein (orange filter) labelling are shown. Arrow, tetracycline; arrow head, calcein. Dynamic histomorphometry parameters calculated from these experiments have been provided in Table 1.

also demonstrates the selectivity of knockdown by the siRNA constructs used for silencing of ERα and ERβ genes. We then investigated mRNA levels of BMP-2 (ER target gene and induced by Med treatment) and collagen Type I (osteoblast differentiation marker), in the presence of selective ER siRNAs. As expected, Med strongly induced BMP-2 mRNA and this increase was abrogated in presence of siERβ but not siERα (Fig. 6E). Further, Med modestly but significantly induced collagen type I mRNA and this effect was abolished in presence of siERβ (Fig. 6F). E2 also exhibited similar pattern (Fig. 6E and F), thus confirming BMP-2 and collagen Type I genes are regulated by ERβ in osteoblasts. Together, from these results, it appears that Med stimulates osteoblast function through activation of ERβ.

3.5. Med promotes modeling-directed bone formation

We next assessed whether Med facilitates skeletal growth in rats. BMCs harvested from the femurs of rats treated with Med (1.0- and 10.0 $mg.kg^{-1}.day^{-1}$ doses) or vehicle was induced for osteoblast mineralization. BMCs harvested from Med-treated rats exhibited dose-dependent increase in the formation of mineralized nodules *ex vivo* compared with vehicle control (Fig. 7A).

Next, dynamic bone formation indices were studied in femur. Fig. 7B shows representative photomicrograph of fluorochrome (tetracycline-calcein) labeling in the femurs of vehicle and Med (10.0 $mg.kg^{-1}.day^{-1}$) treated rats. As 10.0 $mg.kg^{-1}.day^{-1}$ dose resulted in significantly increased formation in the mineralization nodules from BMCs, we assessed dynamic histomorphometric indices from this group of rats. Table 1 shows significant increases in dynamic histomorphometry indices including MS, MAR and BFR, in the femur diaphysis of Med treated rats compared with vehicle treated rats.

Skeletal growth is accompanied by robust cortical bone gain that can be quantitatively determined by μCT. 2D μCT data show significant increases in cortical mean cross-section (B.Ar), periosteal area (T.Ar), periosteal perimeter (T.Pm) and cortical bone perimeter (B.Pm) in the femur diaphysis of Med treated rats compared with controls (Table 2). Increased cortical parameters of femur by Med treatment assessed by static histomorphometry was in agreement with dynamic histomorphometry data.

Biomechanical strength of femur at mid-diaphysis was next evaluated by three-point bending test. Table 3 shows that Med treatment dose-dependently increased force and stiffness of femur, suggesting improved bone quality.

3.6. Assessment of estrogenicity and anti-estrogenicity of Med

Uterine estrogenicity is the major concern for any ER ligand with a therapeutic potential as an osteogenic agent. Since Med activates ER in heterologous system with exogenous ER expression and stimulates osteoblast function via ER, we next examined possible estrogenic effect of Med in uterus. As shown in Fig. 8A, rats treated with either 1.0 or 10.0 $mg.kg^{-1}.day^{-1}$ of Med had histological features comparable to that of control, whereas those treated with E2 exhibited characteristic increase in endometrial hypertrophy with increased cell height. Determination of uterine weight revealed no change between control and Med treated rats, whereas E2-treated rats had significantly higher uterine weight (Table 4). Moreover, ERα (the predominant ER subtype in uterus) [47] is not activated by Med as it has no effect on the expression of an ERα-inducible gene, progesterone receptor (PR) in uterus (Fig. 8B). Interestingly, in MCF-7 (an ER-positive human breast cancer) cells, Med modestly but significantly inhibited cell viability at 10.0 nM and 1.0 μM (Supplementary Fig. S2), suggesting anti-estrogenic effect in breast cancer cells.

Table 1
Dynamic histomorphometric parameters

Bone region	Treatment	Dose, mg/kg	MS, %	MAR, μm/day	BFR, $\mu m^3/\mu m^2$ per day
Femur diaphysis	Vehicle	–	91.81±4.51	1.18±0.04	1.08±0.10
	Med	10	134.3*±6.57	2.01*±0.11	2.69*±0.37

Values represent mean±S.E.M. of three to five observations from each bone section; 8 rats/group.
* $P<.001$, versus corresponding vehicle control group.

Table 2
2-D μCT of femur diaphysis

Treatments	B.Ar.	Cs.Th	T.Ar.	T.Pm.	B.Pm.
Vehicle	1.86±0.102	0.222±0.009	5.51±0.241	9.33±0.254	16.8±0.481
Med (10 mg.kg^{-1})	2.18*±0.018	0.237±0.001	6.59**±0.073	10.1*±0.099	18.4**±0.181

B.Ar, cortical mean cross-section; Cs.Th, cortical thickness, T.Ar, periosteal area; T.Pm, periosteal perimeter; B. Pm, cortical bone perimeter.
* P<.05.
** P<.01 compared with vehicle control. Femur from 6 rats/group was used.

3.7. Systemic bioavailability of Med

Since Med promoted PBM achievement in rats, stimulated osteoblast function via ERβ in vitro and did not exhibit uterine estrogenicity, we thought Med to be worthy of further investigation for osteogenic therapy. To that end, plasma levels of Med were determined in female Sprague–Dawley rats after single oral administration (5.0 mg.kg^{-1} dose). By analyzing maximum plasma concentration (C_{max}) and time to achieve maximum plasma concentration (t_{max}), Med was detected beyond 24 h in plasma (Fig. 9). Area under curve, elimination half-life ($t_{1/2}$) and mean residence time were respectively found to be 395±96 ng.h.ml^{-1}, 5.33 h and 6.959 h. The absolute bioavailability of Med was found to be 22.34%. The metabolite corresponding to equol, as observed in cases of daidzein, was not detected in plasma samples of Med-treated rats.

4. Discussion

The data presented here demonstrate that Med (a methoxylated isoflavonoid) potently stimulates osteoblast differentiation that requires increased ERβ expression and function, promotes parameters of PBM achievement, exhibits good oral bioavailability and is devoid of uterine estrogenicity.

In vitro, Med stimulates differentiation and mineralization of osteoblasts at nanomolar concentrations. Soy isoflavonoids including genistein and daidzein at micromolar concentrations are known to stimulate osteoblast differentiation [48–50]. Med therefore appears to be much more potent than the soy isoflavones, which could be attributed to the presence of methoxy residue in the isoflavonoid ring of Med. Indeed, the presence of methoxy group in the isoflavonoid ring robustly increases potency of osteogenic action has been demonstrated in cases of cajanin (methoxy genistein) and isoformononetin (methoxy daidzein) compared to genistein and daidzein, respectively [32].

We next characterized the cellular signalling events being activated by Med. In ER negative Cos-7 cells with exogenous ER expression, Med, similar to that of E2, transactivated both ERα and β with equal potency. Med also exhibited ER coactivators interaction that was mediated by p38 MAPK. Previous reports suggest that E2 via ER rapidly activates p38 MAPK pathway and this activation plays an integral part in E2-dependent ER–coactivator interactions and related activation of ER target genes via phosphorylation of ER [51–54]. Med appears to mimic E2 signaling events in heterologous system as well as in osteoblasts, so as to trigger a rapid nonnuclear ER-p38 MAPK signaling followed by delayed activation of nuclear event involving ER-BMP-2 pathway, which resulted in the stimulation of osteoblast differentiation.

Table 3
Effect of Med on femoral biomechanical parameters

Treatment	Dose, mg/kg	Ultimate force (N)	Stiffness (N/mm)
Vehicle	–	33.9±1.7	47.8±4.1
Med	1	41.5±3.2	78.8*±10.8
	10	48.5**±2.7	94.7**±8.4

Values represent mean±S.E.M.; n=8.
Crosshead speed for all the tests was 5 mm/min.
* P<.05.
** P<.01 versus corresponding vehicle control group.

Although, Med action in osteoblasts was ER dependent, it had no estrogen-like effect in uterus and did not affect expression of PR, an ERα target gene. Interestingly, in osteoclasts (expressing only ERα), Med induces apoptosis but ICI fails to reverse this effect [29], suggesting that this effect of Med is ER independent. Therefore, it appears that Med functions as a "phyto-SERM" having stimulatory effect in osteoblasts via ER. The selective estrogen receptor modulator (SERM)-like action of Med gains further credence because of its significant anti-proliferative effect in MCF-7 cells, suggesting an anti-estrogenic effect (Supplementary Figure, S2).

Recent evidence suggests that selective activation of the ERβ inhibits breast cancer cell proliferation [55]. As Med increased ERβ but not ERα in osteoblasts, we surmised that Med could mediate its actions in osteoblasts via ERβ. ERβ selectivity of genistein (1.0 μM) has been shown in osteoblast-like U2OS (osteosarcoma) cells in repressing endogenous tumor necrosis factor α (TNFα) gene [29]. Med via ER was found also to inhibit TNFα expression in murine calvarial osteoblasts [29], and similar to that of E2 and genistein, this effect of Med could be mediated by ERβ. ERβ is generally considered to have anti-inflammatory function as it represses proinflammatory genes more effectively than ERα [56]. However, our results that knockdown of ERβ but not ERα abrogates Med-induced osteoblast differentiation genes (BMP-2 and Type I collagen) demonstrate that ERβ could also promote osteogenic genes and stimulate osteoblast function. As Med transactivates both ERα and ERβ with similar potency (Fig. 3A,B), stimulation of osteoblast function by Med could be mediated by increasing ERβ levels in these cells. Role of ERβ in the regulation of E2-induced osteogenic genes have been reported in human peridontal ligament cells [57] and MG-63 osteosarcoma cells [58], although whether E2 increased ERβ protein levels in those cells have not been described. Based on our results, it is reasonable to assume that E2 or phytoestrogens (such as Med and other isoflavonoids) stimulate osteoblast function by up-regulating ERβ levels in osteoblasts. Indeed, genistein and daidzein whose affinities for ERβ are greater than that for ERα, have been found to promote osteogenesis [13,59,60]. However, Med appears to be more potent in stimulating osteoblast function than other isoflavonoids such as genistein, daidazein or biochanin-A.

In vivo Med has osteogenic effect in growing rats wherein modeling-directed bone formation led to higher PBM achievement. In rats, PBM is attained between 3 and 12 months of postnatal age [61]. We gave Med treatment for 4 weeks after weaning when final PBM was yet to be attained. Since isoflavones and their derivatives are classified as phytoestrogens, it was deemed reasonable to avoid the introduction of estrogen effect on growing skeleton in rats so that it did not obscure the effect of Med. "Vaginal opening" marks commencement of estrogen function in rats, and our study ensured termination before this event.

Under the circumstance of estrogen-independent skeletal growth, Med treatment resulted in dose-dependent increase in mineralization of BMCs in comparison to control, thus suggesting increased

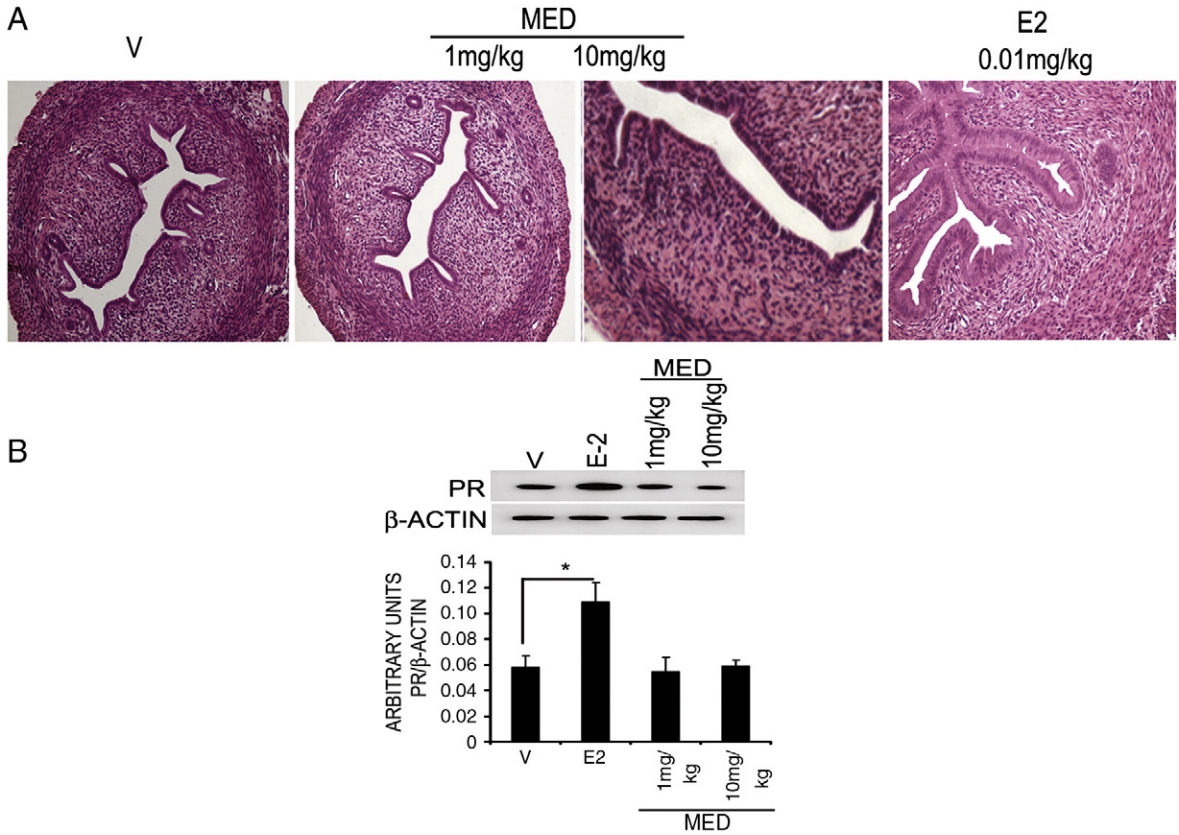

Fig. 8. Med is devoid of uterine estrogenecity. (A) Uteri were harvested from rats treated with various substances. Cross-sections of uterine tissues were stained with H&E, and sections were examined for histomorphometry. For additional data, refer to Table 4. (B) Uteri were harvested from rats treated with E2 or Med, and Western blot against PR or β-actin were performed, one representative blot is shown in the upper panel. Lower panel shows densitometric analysis of Western blots. Data represent mean±S.E. from three independent experiments. *P<.05.

osteogenic differentiation of bone marrow osteoprogenitor cells. An increased differentiation of BMCs to osteoprogenitor cells is expected to favor bone formation [29]. Indeed, we observed increased MS (a function of increased osteoblast differentiation) and MAR and BFR (resulting from expansion of bone marrow osteoblast pool) in femur diaphysis of Med treated rats compared with controls by dynamic histomorphometry. Moreover, in agreement with dynamic histomorphometry data, μCT (static histomorphometry) results demonstrated increased cortical bone gain by Med during the course of skeletal growth in rats compared with controls. Further, increased femur periosteal bone deposition by Med had functional consequence in increasing bone biomechanical strength as Med dose-dependently increased femoral force and stiffness. Together, our data so far suggest that Med stimulates osteoblast function in vitro and bone formation in vivo thus facilitating skeletal growth.

Bioavailability is an important determinant of in vivo efficacy of any compound. Phytoestrogens in general suffer from poor oral bioavailability [62]. The oral bioavailability is dependent on absorption and systemic clearance, which in turn depend on lipophilicity of the molecules. It is reported that the *O*-methylation of free phenolic hydroxyl groups enhances the lipophilicity and leads to derivatives not susceptible to glucuronic acid or sulfate conjugation, resulting in increased metabolic stability [63]. Med is structurally akin to *O*-methylated isoflavonoid. We observed that Med has 22.34% oral bioavailability suggesting adequate metabolic stability. The prolonged systemic exposure of Med and plasma half life of 5.33 h indicate that once a day dosage regimen is sufficient to maintain the effective plasma concentration for its osteogenic effect in vivo. Moreover, Med does not produce equol, a highly estrogenic metabolite. As the bioactivity of the most abundant soy isoflavonoid, daidzein is dependent on its intestinal biotransformation to equol and since 40% humans lack this conversion machinery, the beneficial skeletal effect of Med is expected to include the so called "equol nonresponder" group.

Table 4
Effect of Med on uterine wet weight

Treatments	Dose (mg.kg^{-1})	Uterine weight (mg)	% Gain
Vehicle	–	14.7±2.2	–
E2	0.01	98.3*±11.5	568*
Med	1	18.8±2.9	28 (N.S.)
Med	10	20.0±1.6	36 (N.S.)

Values are mean±S.E.M. of eight rats per group.
N.S., not significant.
* P<.001 versus corresponding vehicle control group.

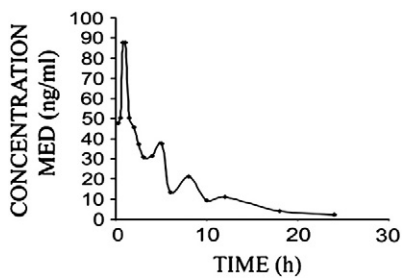

Fig. 9. Plasma concentration-time profile of Med after a single oral dose of 5.0 mg.kg^{-1} Med to female Sprague–Dawley rats. Data are described in Section 3.7.

Collectively, we demonstrate that Med promotes PBM achievement and likely acts via ERβ in osteoblasts. Based on our data, nutraceutical supplement of Med for optimum skeletal growth is suggested. In addition, favourable pharmacokinetic profile of Med suggests its therapeutic potential in postmenopausal osteoporosis although it requires experimental validation in appropriate animal model, for example in ovariectomized rats that have developed osteopenia. Finally, further understanding of the mechanism of ERβ stimulatory action of Med in osteoblasts may lead to development of safer and more potent SERM having osteogenic effect.

Acknowledgments

Authors gratefully acknowledge generous funding from the Ministry of Health and Family Welfare (grant-in-aid); Council of Scientific and Industrial Research (NWP0034); the Department of Biotechnology (S.S.); the Department of Science and Technology (D.S.); and the Indian Council of Medical Research (N.C.).

Appendix A. Supplementary data

Supplementary materials related to this article can be found online at doi:10.1016/j.jnutbio.2010.11.002.

References

[1] Bonjour JP, Chevalley T, Ferrari S, Rizzoli R. The importance and relevance of peak bone mass in the prevalence of osteoporosis. Salud Publica Mex 2009;51(Suppl 1):S5–S17.
[2] Seeman E, Tsalamandris C, Formica C. Peak bone mass, a growing problem? Int J Fertil Menopausal Stud 1993;38(Suppl 2):77–82.
[3] Kelsey JL. Risk factors for osteoporosis and associated fractures. Public Health Rep 1989;104(Suppl):14–20.
[4] Cooper C, Harvey N, Cole Z, Hanson M, Dennison E. Developmental origins of osteoporosis: the role of maternal nutrition. Adv Exp Med Biol 2009;646:31–9.
[5] Cooper C, Harvey N, Javaid K, Hanson M, Dennison E. Growth and bone development. Nestle Nutr Workshop Ser Pediatr Program 2008;61:53–68.
[6] Malhotra N, Mithal A. Osteoporosis in Indians. Indian J Med Res 2008;127:263–8.
[7] Uesugi T, Fukui Y, Yamori Y. Beneficial effects of soybean isoflavone supplementation on bone metabolism and serum lipids in postmenopausal Japanese women: a four-week study. J Am Coll Nutr 2002;21:97–102.
[8] Picherit C, Coxam V, Bennetau-Pelissero C, Kati-Coulibaly S, Davicco MJ, Lebecque P, et al. Daidzein is more efficient than genistein in preventing ovariectomy-induced bone loss in rats. J Nutr 2000;130:1675–81.
[9] Mardon J, Mathey J, Kati-Coulibaly S, Puel C, Davicco MJ, Lebecque P, et al. Influence of lifelong soy isoflavones consumption on bone mass in the rat. Exp Biol Med (Maywood) 2008;233:229–37.
[10] Coxam V. Phyto-oestrogens and bone health. Proc Nutr Soc 2008;67:184–95.
[11] Ho SC. Soy intake and the maintenance of peak bone mass in Hong Kong Chinese women. Journal of Bone and Mineral Research 2001;16:1363–9.
[12] Setchell KDR, Brown NB, Lydeking-Olsen E. The clinical significance of the metabolite equol:a clue to the effectiveness of soy and its isoflavones. Journal of Nutrition 2002;132:3577–84.
[13] Chen W, Lin Z, Ning M, Yang C, Yan X, Xie Y, et al. Aza analogues of equol: novel ligands for estrogen receptor beta. Bioorg Med Chem 2007;15:5828–36.
[14] Wu J, Oka J, Ezaki J, Ohtomo T, Ueno T, Uchiyama S, et al. Possible role of equol status in the effects of isoflavone on bone and fat mass in postmenopausal Japanese women: a double-blind, randomized, controlled trial. Menopause 2007;14:866–74.
[15] Elizabeth Brink VC, Robins S, Wahala K, Cassidy A, Branca F. Long-term consumption of isoflavone-enriched foods does not affect bone mineral density, bone metabolism, or hormonal status in early postmenopausal women: a randomized, double-blind, placebo controlled study. Am J Clin Nutr 2008;87:761–70.
[16] Kenny AM, Mangano KM, Abourizk RH, Bruno RS, Anamani DE, Kleppinger A, et al. Soy proteins and isoflavones affect bone mineral density in older women: a randomized controlled trial. Am J Clin Nutr 2009;90:234–42.
[17] Wong WW, Lewis RD, Steinberg FM, Murray MJ, Cramer MA, Amato P, et al. Soy isoflavone supplementation and bone mineral density in menopausal women: a 2-y multicenter clinical trial. Am J Clin Nutr 2009;90:1433–9.
[18] Robinson LJ, Yaroslavskiy BB, Griswold RD, Zadorozny EV, Guo L, Tourkova IL, et al. Estrogen inhibits RANKL-stimulated osteoclastic differentiation of human monocytes through estrogen and RANKL-regulated interaction of estrogen receptor-alpha with BCAR1 and Traf6. Exp Cell Res 2009;315:1287–301.
[19] Lee K, Jessop H, Suswillo R, Zaman G, Lanyon L. Endocrinology: bone adaptation requires oestrogen receptor-alpha. Nature 2003;424:389.
[20] van der Eerden BC, Lowik CW, Wit JM, Karperien M. Expression of estrogen receptors and enzymes involved in sex steroid metabolism in the rat tibia during sexual maturation. J Endocrinol 2004;180:457–67.
[21] Barz W, Daniel S, Hinderer W, Jaques U, Kessmann H, Koster J, et al. Metabolism and enzymology of isoflavone malonylglucosides and pterocarpan phytoalexins in cicer arietinum. Planta Med 1986;52:420.
[22] Liu CJ, Deavours BE, Richard SB, Ferrer JL, Blount JW, Huhman D, et al. Structural basis for dual functionality of isoflavonoid *O*-methyltransferases in the evolution of plant defense responses. Plant Cell 2006;18:3656–69.
[23] Miao VP, Vanetten HD. Three genes for metabolism of the phytoalexin maackiain in the plant pathogen *Nectria haematococca*: meiotic instability and relationship to a new gene for pisatin demethylase. Appl Environ Microbiol 1992;58:801–8.
[24] Marais JPJDB, Dixon RA, Ferreira D. The stereochemistry of flavonoids. In: Grotewold, editor. The science of flavonoids. Springer Science+Business Inc; 2006. p. 1–46.
[25] Guo L, Paiva NL. Molecular cloning and expression of alfalfa (*Medicago sativa* L.) vestitone reductase, the penultimate enzyme in medicarpin biosynthesis. Arch Biochem Biophys 1995;320:353–60.
[26] Kaufman PB, Duke JA, Brielmann H, Boik J, Hoyt JE. A comparative survey of leguminous plants as sources of the isoflavones, genistein and daidzein: implications for human nutrition and health. J Altern Complement Med 1997;3:7–12.
[27] Booth NL, Overk CR, Yao P, Burdette JE, Nikolic D, Chen SN, et al. The chemical and biologic profile of a red clover (*Trifolium pratense* L.) phase II clinical extract. J Altern Complement Med 2006;12:133–9.
[28] Maurya R, Yadav DK, Singh G, Bhargavan B, Narayana Murthy PS, Sahai M, et al. Osteogenic activity of constituents from *Butea monosperma*. Bioorg Med Chem Lett 2009;19:610–3.
[29] Tyagi AMGA, Kumar A, Srivastava K, Bhargavan B, Trivedi R, Saravanan S, et al. Medicarpin inhibits osteoclastogenesis and has nonestrogenic bone conserving effect in ovariectomized mice. Mol Cell Endocrinol 2010;325:101–9.
[30] Sanyal S, Bavner A, Haroniti A, Nilsson LM, Lundasen T, Rehnmark S, et al. Involvement of corepressor complex subunit GPS2 in transcriptional pathways governing human bile acid biosynthesis. Proc Natl Acad Sci U S A 2007;104:15665–70.
[31] Heldring N, Nilsson M, Buehrer B, Treuter E, Gustafsson JA. Identification of tamoxifen-induced coregulator interaction surfaces within the ligand-binding domain of estrogen receptors. Mol Cell Biol 2004;24:3445–59.
[32] Bhargavan B, Gautam AK, Singh D, Kumar A, Chaurasia S, Tyagi AM, et al. Methoxylated isoflavones, cajanin and isoformononetin, have non-estrogenic bone forming effect via differential mitogen activated protein kinase (MAPK) signaling. J Cell Biochem 2009;108:388–99.
[33] Gautam AKBB, Tyagi AM, Srivastava K, Yadav DK, Kumar M, Singh A, et al. Differential effects of formononetin and cladrin on osteoblast function, peak bone mass achievement and bioavailability in rats. J Nutr Biochem 2010 [Epub ahead of print].
[34] Trivedi R, Kumar A, Gupta V, Kumar S, Nagar GK, Romero JR, et al. Effects of Egb 761 on bone mineral density, bone microstructure, and osteoblast function: Possible roles of quercetin and kaempferol. Mol Cell Endocrinol 2009;302:86–91.
[35] Trivedi R, Kumar S, Kumar A, Siddiqui JA, Swarnkar G, Gupta V, et al. Kaempferol has osteogenic effect in ovariectomized adult Sprague–Dawley rats. Mol Cell Endocrinol 2008;289:85–93.
[36] Kumar ASA, Gautam AK, Chandra D, Singh D, Changkija B, Singh MP, et al. Identification of kaempferol-regulated proteins in rat calvarial osteoblasts during mineralization by proteomics. Proteomics 2010;10:1730–9.
[37] Gregory CA, Gunn WG, Peister A, Prockop DJ. An Alizarin red-based assay of mineralization by adherent cells in culture: comparison with cetylpyridinium chloride extraction. Anal Biochem 2004;329:77–84.
[38] Fujioka M, Sudo Y, Okumura M, Wu J, Uehara M, Takeda K, et al. Differential effects of isoflavones on bone formation in growing male and female mice. Metabolism 2007;56:1142–8.
[39] Pandey R, Gautam AK, Biju B, Trivedi R, Swarnkar G, Nagar GK, et al. Total extract and standardized fraction from the 1 stem-bark of *Butea monosperma* have osteoprotective action: evidence for the non-estrogenic osteogenic effect of the standardized fraction. Menopause 2010;17:602–10.
[40] Hara K, Kobayashi M, Akiyama Y. Vitamin K2 (menatetrenone) inhibits bone loss induced by prednisolone partly through enhancement of bone formation in rats. Bone 2002;31:575–81.
[41] Sharan K, Siddiqui JA, Swarnkar G, Tyagi AM, Kumar A, Rawat P, et al. Extract and fraction from Ulmus wallichiana Planchon promote peak bone achievement and have a nonestrogenic osteoprotective effect. Menopause 17:393-402.
[42] Srivastava SR, Keshri G, Bhargavan B, Singh C, Singh MM. Pregnancy interceptive activity of the roots of *Calotropis gigantea* Linn. in rats. Contraception 2007;75:318–22.
[43] Shimo T, Matsumura S, Ibaragi S, Isowa S, Kishimoto K, Mese H, et al. Specific inhibitor of MEK-mediated cross-talk between ERK and p38 MAPK during differentiation of human osteosarcoma cells. J Cell Commun Signal 2007;1:103–11.
[44] Zhou S, Turgeman G, Harris SE, Leitman DC, Komm BS, Bodine PV, et al. Estrogens activate bone morphogenetic protein-2 gene transcription in mouse mesenchymal stem cells. Mol Endocrinol 2003;17:56–66.
[45] Yin H, Glass J, Blanchard KL. MOZ-TIF2 repression of nuclear receptor-mediated transcription requires multiple domains in MOZ and in the CID domain of TIF2. Mol Cancer 2007;6:51.
[46] Bonnelye E, Aubin JE. Differential expression of estrogen receptor-related receptor alpha and estrogen receptors alpha and beta in osteoblasts in vivo and in vitro. J Bone Miner Res 2002;17:1392–400.

[47] Pelletier G. Localization of androgen and estrogen receptors in rat and primate tissues. Histol Histopathol 2000;15:1261–70.
[48] Jia TL, Wang HZ, Xie LP, Wang XY, Zhang RQ. Daidzein enhances osteoblast growth that may be mediated by increased bone morphogenetic protein (BMP) production. Biochem Pharmacol 2003;65:709–15.
[49] Liao QC, Xiao ZS, Qin YF, Zhou HH. Genistein stimulates osteoblastic differentiation via p38 MAPK-Cbfa1 pathway in bone marrow culture. Acta Pharmacol Sin 2007;28:1597–602.
[50] Pan W, Quarles LD, Song LH, Yu YH, Jiao C, Tang HB, et al. Genistein stimulates the osteoblastic differentiation via NO/cGMP in bone marrow culture. J Cell Biochem 2005;94:307–16.
[51] Frigo DE, Basu A, Nierth-Simpson EN, Weldon CB, Dugan CM, Elliott S, et al. p38 mitogen-activated protein kinase stimulates estrogen-mediated transcription and proliferation through the phosphorylation and potentiation of the p160 coactivator glucocorticoid receptor-interacting protein 1. Mol Endocrinol 2006;20:971–83.
[52] Lee H, Bai W. Regulation of estrogen receptor nuclear export by ligand-induced and p38-mediated receptor phosphorylation. Mol Cell Biol 2002;22:5835–45.
[53] Mori-Abe A, Tsutsumi S, Takahashi K, Toya M, Yoshida M, Du B, et al. Estrogen and raloxifene induce apoptosis by activating p38 mitogen-activated protein kinase cascade in synthetic vascular smooth muscle cells. J Endocrinol 2003;178:417–26.
[54] Cheskis BJ, Greger J, Cooch N, McNally C, McLarney S, Lam HS, et al. MNAR plays an important role in ERa activation of Src/MAPK and PI3K/Akt signaling pathways. Steroids 2008;73:901–5.
[55] Hartman J, Lindberg K, Morani A, Inzunza J, Strom A, Gustafsson JA. Estrogen receptor beta inhibits angiogenesis and growth of T47D breast cancer xenografts. Cancer Res 2006;66:11207–13.
[56] An JRR, Webb P, Gustafsson JA, Kushner PJ, Baxter JD, Leitman DC. Estradiol repression of tumor necrosis factor-alpha transcription requires estrogen receptor activation function-2 and is enhanced by coactivators. Proc Natl Acad Sci U S A 1999;96:15161–6.
[57] Liang L, Yu JF, Wang Y, Wang G, Ding Y. Effect of estrogen receptor beta on the osteoblastic differentiation function of human periodontal ligament cells. Arch Oral Biol 2008;53:553–7.
[58] Cao L, Bu R, Oakley JI, Kalla SE, Blair HC. Estrogen receptor-beta modulates synthesis of bone matrix proteins in human osteoblast-like MG63 cells. J Cell Biochem 2003;89:152–64.
[59] Yamaguchi M, Sugimoto E. Stimulatory effect of genistein and daidzein on protein synthesis in osteoblastic MC3T3-E1 cells: activation of aminoacyl-tRNA synthetase. Mol Cell Biochem 2000;214:97–102.
[60] Sugimoto E, Yamaguchi M. Anabolic effect of genistein in osteoblastic MC3T3-E1 cells. Int J Mol Med 2000;5:515–20.
[61] Ke HZ, Crawford DT, Qi H, Chidsey-Frink KL, Simmons HA, Li M, et al. Long-term effects of aging and orchidectomy on bone and body composition in rapidly growing male rats. J Musculoskelet Neuronal Interact 2001;1:215–24.
[62] Setchell KD, Zhao X, Jha P, Heubi JE, Brown NM. The pharmacokinetic behavior of the soy isoflavone metabolite S-(−)equol and its diastereoisomer R-(+)equol in healthy adults determined by using stable-isotope-labeled tracers. Am J Clin Nutr 2009;90:1029–37.
[63] Walle T. Methylation of dietary flavones increases their metabolic stability and chemopreventive effects. Int J Mol Sci 2009;10:5002–19.